Thermodynamics of hydrogen release in complexed borohydrides

D. Harrison and T. Thonhauser*
Department of Physics, Wake Forest University, Winston-Salem, North Carolina 27109, USA
and Center for Functional Materials, Wake Forest University, Winston-Salem, North Carolina 27109, USA

(Received 29 December 2017; revised manuscript received 26 April 2018; published 20 June 2018)

An important aspect of successful hydrogen storage materials is their hydrogen release mechanism, which—unfortunately—for many promising materials occurs at impractically high or low temperatures. In light of recent improvements observed when complexing borohydrides with NH_3, we performed an *ab initio* investigation into the effects of complexing the borohydrides $Al(BH_4)_3$, $Mg(BH_4)_2$, and $Zn(BH_4)_2$ with new additive molecules CH_4, C_2H_6O, and H_2O, as well as NH_3 as a benchmark. To find candidate ground-state structures for these borohydride complexes, we first performed an in-depth evolutionary structure search. These ground-state structures were then used to both evaluate their thermodynamic properties as well as to investigate nearby metastable states that facilitate a favorable hydrogen release using evolutionary metadynamics. We found that all of these additives markedly affect—to a varying degree—the nearby metastable states relative to the unaltered borohydride. Furthermore, we found that complexing borohydrides with CH_4 and H_2O results in particularly favorable properties for improving their hydrogen release. Our study not only investigates new and promising hydrogen storage materials, but also elucidates the hydrogen release mechanism and the effect of additives in processes that are difficult to characterize experimentally.

DOI: 10.1103/PhysRevMaterials.2.065403

I. INTRODUCTION

Hydrogen is considered an ideal alternative to fossil fuels due to its potential to be produced and consumed cleanly and renewably [1–3]. Unfortunately, under ambient conditions, hydrogen has very low volumetric density, making it unsuitable for automotive applications. This has led to a wealth of research on improving hydrogen storage methods in general [4,5], with goals outlined by the US Department of Energy (DOE) [6,7]. Of particular interest for hydrogen storage is the class of borohydride materials—which are complex hydrides formed from a cationic metal and an anionic BH_4 group—due to their favorably high gravimetric and volumetric hydrogen densities. Unfortunately, their hydrogen desorption temperatures are typically well above 85 °C [8,9], i.e., the maximum delivery temperature set by the DOE for fuel cell operation in vehicles [7]. Research efforts concerning borohydrides have thus mostly focused on improving their hydrogen-release properties [6,10–17].

Examples of past research to improve borohydride properties include destabilizing via reactions with other hydrides [18–21], alloying [22–24], cation substitution [25], anion substitution [26], and adding catalysts [27]. In general, the goal of most of these methods is to lower the hydrogen desorption temperature by altering either the kinetics or thermodynamics of the reaction. One particularly successful method is the complexing of borohydrides with additional molecules such as ammonia (NH_3) [28–34]. The effect of introducing ammonia into borohydrides depends somewhat on the particular borohydride, but it is almost always beneficial. For borohydrides which are too stable (i.e., the temperature at which they release hydrogen is too high), ammonia complexing has been found to decrease the hydrogen release temperature remarkably; for borohydrides which are too unstable (i.e., the temperature at which they release hydrogen is too low), ammonia complexing has been found to increase the release temperature [30,34]. In a recent study, we have uncovered the mechanisms behind both of those findings [35].

Because of the beneficial effects of ammonia complexing in borohydrides, in the present work we investigate the effects of complexing borohydrides with other small molecules. In particular, we investigate the effects of complexing $Al(BH_4)_3$ [36,37], $Mg(BH_4)_2$ [38,39], and $Zn(BH_4)_2$ [29,40,41] with H_2O, CH_4, C_2H_6O, and NH_3. These borohydrides were chosen so as to have a representative range of stabilities and structures out of the class of borohydrides [9]. The small molecules were chosen so as to have a range of polarity and size. We included NH_3 in our study as a benchmark for which a myriad of experimental data exists [28–33].

To fully capture the effects of complexing borohydrides, the thermodynamics and kinetics of the resulting phases have to be investigated. While the former is fairly straightforward within *ab initio* materials modeling, the latter is almost prohibitively complex. Although basic transition-state search algorithms exist that can in principle find kinetic barriers [42,43], the problem is that, even in simple borohydrides, the release mechanism can be very complex, forming such intermediates as $B_{12}H_{12}$ and involving several steps [44]. Similarly, while *ab initio* molecular dynamics (AIMD) could theoretically be employed to study the hydrogen release process, in practice the large energy barriers to these processes make the actual hydrogen release a rare event on the timescale accessible to AIMD. Considering that many borohydrides have a sluggish

*thonhauser@wfu.edu

hydrogen release anyway, the required timescale for AIMD is far beyond reach by several orders of magnitude. While there are a number of strategies for dealing with this situation [45], we focus here on metadynamics, i.e., a technique to sample rare events by adding cumulative Gaussian energy penalties to regions of phase space that have already been explored. This technique provides a means to sample rare events within systems which otherwise would be unobservable due to their large activation energy. A fairly recent innovation to this technique is known as *evolutionary metadynamics* [46,47], a discussion of which is provided in the Appendix. We have used this novel technique to investigate nearby metastable states and the effect of complexing on them to deduce information about the hydrogen release characteristics. In conjunction with the Bell–Evans–Polanyi principle of physical chemistry [48,49]—wherein the difference in activation energy between two reactions is proportional to the difference of their enthalpy of reaction—we obtain crucial insights into the mechanisms for the initial steps in the borohydride decomposition, including the effect that additive molecules have upon these steps.

II. COMPUTATIONAL DETAILS

A. *Ab initio* ground-state calculations

We performed *ab initio* simulations at the density functional theory (DFT) level as implemented in VASP [50,51] using the standard projector augmented wave (PAW) pseudopotentials provided. A plane-wave energy cutoff of 520 eV and k-point mesh density of 0.08 $Å^{-1}$ were used. The energy convergence criterion and force criterion were varied depending on the level of accuracy desired for the method employed, with specific details outlined in the corresponding sections below. As previous studies on borohydrides found that van der Waals interactions are crucial to accurately model these materials due to weak interactions between the BH_4 units [37,52,53], we employed the exchange-correlation functional vdW-DF [54–57], which includes a truly nonlocal correlation term to capture van der Waals binding.

B. Ground-state structures and structure searches

To study borohydrides with additive molecules, it was first necessary to determine their corresponding ground-state structures. To this end, we used the crystal structure prediction program USPEX [58–61] in combination with VASP. USPEX was configured to run a three-dimensional molecular structure search with a population size of 10 at each generation. The structure search was stopped if the same structure had the lowest energy for 6 generations in a row or if a total of 30 generations were ran. Three molecules were used in each structure search: the borohydride molecule (BH_4), the metal (Al, Mg, or Zn), and the additive molecule (CH_4, C_2H_6O, H_2O, or NH_3); one formula unit was used for both the borohydride and the additive molecule. For example, for the complexed $Al(BH_4)_3 \cdot NH_3$ structure, a molecular structure search was performed with one Al, one NH_3 molecule, and three BH_4 molecules. While it is possible that the true ground-state structures contain additional formula units, we argue in Sec. IV C that the determining factor for the properties of the complexed phases is that they have been complexed at all. The best structures from each structure search were relaxed by using an electronic convergence of 10^{-7} eV until all forces were less than 10^{-3} eV/Å. Throughout the entire structure search a total of 1780 structures were evaluated.

In addition, the energies of the elements, additive molecules, and pure borohydrides were calculated by using the same criteria. For those elements or molecules which exist in the gaseous phase under standard conditions (e.g., H_2), a $10 \times 10 \times 10$ Å box was used. From this, we then computed thermodynamic properties of these structures, finding both their enthalpy of formation and the enthalpy of reaction to form the borohydride complex from the borohydride molecules and the additive molecules. Our previous study on borohydrides showed that vibrational contributions to the relative differences in formation enthalpy are negligible (e.g., the zero-point-energy contribution is $\sim$0.4 eV/BH_4 regardless of the metal for Mg, Zn, Al, and Sc borohydrides) [62,63], so those effects were not included in the present study.

For the pure borohydride structures, we did not perform a structure search, as their ground-state structures were already known, but instead used the listed known structures. The structure used for $Al(BH_4)_3$ was the solid-phase β-$Al(BH_4)_3$ taken from the theoretical work of Miwa *et al.* [37,64], the structure for $Zn(BH_4)_2$ was taken from Nakamori *et al.* [8], the structure for boron was the 106 atom β-rhombohedral structure suggested by van Setten *et al.* [65], and the structure used for $Mg(BH_4)_2$ was the 99-atom structure found to be nearly isoenergetic to the true ground-state structure (which was not used due to its large unit cell with 330 atoms) [53].

C. Metastable structures

To generate a host of metastable structures, we again used USPEX in conjunction with VASP, although this time utilizing the evolutionary metadynamics method [46,47]. For the borohydride-additive structures, the starting structures used were $2 \times 2 \times 2$ supercells (such that each structure had eight formula units) created from the structures found through the initial structure search. Supercells were created for these structures in order to lessen interactions among periodic images when the structure is perturbed. No supercells were created for the pure borohydride structures because they already contained several formula units per unit cell. At each generation, a population size of 10 structures was used. The Gaussian penalty height and width used were 16 000 $Å^3$ kbar and 1.6 Å, respectively. Cell size and shape were allowed to vary and the structures were relaxed by using an electronic convergence of 10^{-5} eV until all forces were less than 0.1 eV/Å. Due to the large unit-cell sizes only the Γ point was used for all metastable structure calculations. For each structure, at least six generations were performed. In total, we have generated and evaluated 1448 different metastable structures.

III. THERMODYNAMICS RESULTS OF COMPLEXING BOROHYDRIDES

As the first step in our investigation of the effect of complexing borohydrides, we compute their thermodynamical properties. Figure 1 shows the formation enthalpies for all borohydride-additive combinations, including no additive as

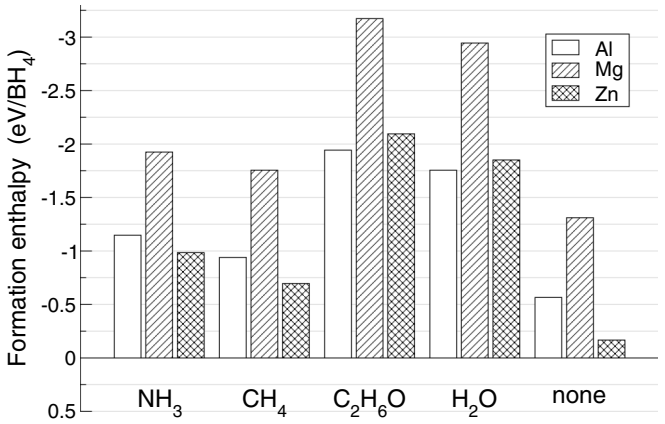

FIG. 1. Formation enthalpies ΔH_f in eV/BH_4 for $\mathcal{M}(BH_4)_n \cdot \mathcal{X}$ for $\mathcal{M}$ = Al, Mg, Zn and $\mathcal{X} = NH_3$, CH_4, C_2H_6O, H_2O. The pure borohydrides without any additives are shown under "none."

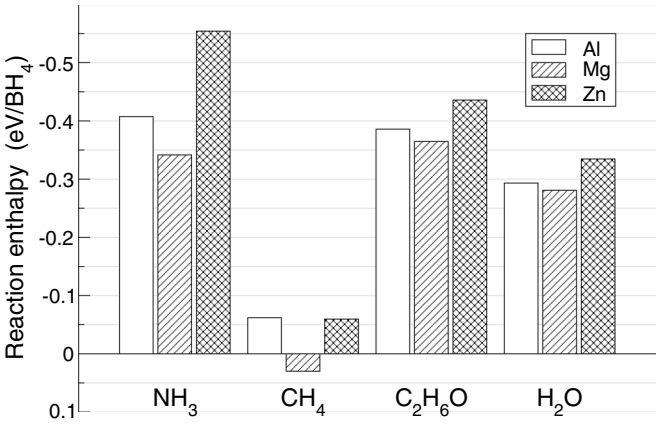

FIG. 2. Reaction enthalpy ΔH_r in eV/BH_4 to form the complexed borohydride, i.e., $\mathcal{M}(BH_4)_n + \mathcal{X} \rightarrow \mathcal{M}(BH_4)_n \cdot \mathcal{X}$ for $\mathcal{M}$ = Al, Mg, Zn and $\mathcal{X} = NH_3$, CH_4, C_2H_6O, H_2O. Negative values indicate a favorable reaction.

a reference. Overall, these results confirm that all of the structures studied are stable with respect to decomposition to the elements. It also becomes immediately clear that the additives in all cases increase the stability of the materials.

More interestingly, we recently developed a criterion for determining whether a borohydride will produce diborane—an undesirable byproduct that is poisonous to the fuel cell—upon decomposition, based on the formation enthalpy of the borohydride [63]. In particular, we showed that, for values greater than ~ -1.1 eV/BH_4, diborane will be produced; while this criterion was developed in the context of pure borohydrides, there is evidence which suggests it may be more generally applicable [29,63]. We thus predict that all additives to some degree suppress diborane production during the hydrogen release (albeit not necessarily reaching the -1.1 eV/BH_4 threshold under the additive concentration studied), with H_2O and C_2H_6O providing the greatest degree of suppression.

To further investigate the stability of borohydride-additive combinations, we also calculate the energy gained from combining the borohydride and its additive, i.e., the reaction enthalpy to form the complexed borohydride

$$\mathcal{M}(BH_4)_n + \mathcal{X} \longrightarrow \mathcal{M}(BH_4)_n \cdot \mathcal{X} \qquad (1)$$

for the various combinations of metals $\mathcal{M}$ and additives $\mathcal{X}$. The results depicted in Fig. 2 reveal two clear trends: (i) The NH_3, C_2H_6O, and H_2O additives result in very stable compounds, whereas CH_4 produces less stable complexed borohydrides. This finding can be explained in terms of the polarity of the additives: The polarity of NH_3, C_2H_6O, and H_2O enable them to bind stronger with the anions and cations in the borohydride than with the nonpolar CH_4. Note that, when CH_4 is combined with $Mg(BH_4)_2$, the overall compound is predicted to be slightly unstable with respect to phase segregation, although not so much so that the phase could not be stabilized kinetically or due to the entropy of mixing. (ii) The relative stability of an additive is inversely proportional to the stability of the borohydride, a trend that we will again see in the discussion of the metadynamics results. In other words, as seen by referencing the pure borohydride formation enthalpies (Fig. 1 under "none"), the least stable borohydrides [e.g., $Zn(BH_4)_2$] have the strongest affinity for additive molecules.

IV. METADYNAMICS RESULTS OF COMPLEXING BOROHYDRIDES

A. The idea and implicit assumptions behind metadynamics

Starting from a suitable collection of accurate structures both for pure borohydrides and borohydride complexes, evolutionary metadynamics allows us to take these structures as input and catalog the energy and composition of a large number of nearby metastable states for these structures as output. Our goal in doing this is to study the first critical steps in the decomposition of a borohydride and use these to help us understand what relation exists (if any) between these first steps and the full decomposition (by comparing with known experimental results), as well as determine the effects additives have on these initial decomposition steps.

As an example, it is known that complexing $Mg(BH_4)_2$ with NH_3 decreases the temperature of hydrogen release [66]. This phenomenon is the result of NH_3 lowering the energy barrier for hydrogen production [35]. To find this behavior within the realm of evolutionary metadynamics, we would look at the reaction enthalpy of resultant metastable structures which contain H_2 molecules for pure $Mg(BH_4)_2$ and compare that to the reaction enthalpy of resultant metastable structures which contain H_2 molecules for $Mg(BH_4)_2 \cdot NH_3$. Of course, the thermodynamics of the metastable states by itself cannot directly reveal information about the kinetics of the hydrogen release. But it provides valuable insight in that the *difference* in reaction barriers between two such reactions is proportional to the *difference* of their reaction enthalpy, a relationship called the Bell–Evans–Polanyi principle of physical chemistry [48,49]. We argue that this principle is applicable here based on comparing with explicit calculations of reaction barriers through a transition-state search algorithm for diborane production in several borohydrides [35]. These calculations also reveal that the difference in reaction enthalpy for two metastable states is typically only on the order of 10% of the overall reaction barrier.

Finally, we also would like to emphasize that, while in our study we have investigated nearby metastable states to the ground-state structures of borohydrides and

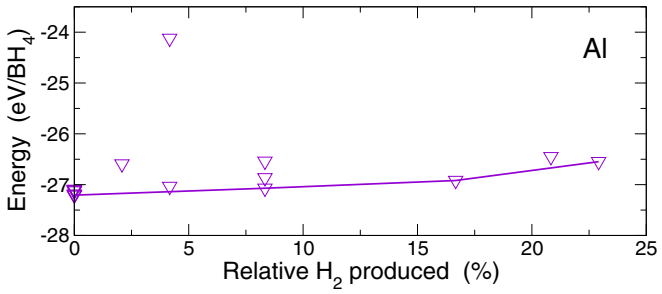

FIG. 3. Example plot showing energy vs relative H_2 concentration for the best structures at each generation found by the evolutionary metadynamics structure search for $Al(BH_4)_3 \cdot NH_3$. The purple line represents the bottom part of the convex hull, illustrating the technique used to develop all following plots.

borohydride-additive complexes, the full decomposition reaction includes several additional steps which include both further decomposition of the structure and the diffusion of hydrogen (and possibly other gases, such as diborane) from the bulk material. Our implicit assumption in comparing our metadynamics results to experimental results is that the initial steps in the decomposition reaction directly affect the full decomposition. This would be the case, e.g., if the initial steps are the rate-limiting steps in the reaction. On the other hand, while the exact processes and barriers for the full decomposition reactions remain unknown, the fact that there is good agreement between our metadynamics results and experimental data suggests that the initial decomposition reaction steps are critical for determining the pathway for the full decomposition pathway.

B. An example: $Al(BH_4)_3 \cdot NH_3$

To better understand our analysis of the metastable states in the next section, we present here, as an example, the case of $Al(BH_4)_3 \cdot NH_3$ in more detail. Figure 3 shows a plot of relative stability vs H_2 concentration for the best structures produced by USPEX from the evolutionary metadynamics simulation. The y axis is defined as the energy of these structures in eV/BH_4 while the x axis is defined as the number of hydrogens in H_2 molecules divided by the total number of hydrogens originally contained in the BH_4 molecules (we only count individual H_2 molecules, i.e., two hydrogen atoms that are exclusively bound to each other and that are not part of a larger molecule). For example, for our $2 \times 2 \times 2$ supercell of $Al(BH_4)_3 \cdot NH_3$ with eight formula units, eight H_2 molecules would have a relative H_2 concentration of 16.67%, because there are 96 total hydrogens in the 24 BH_4 units. As another example, if the entire hydrogen in all BH_4 units was released as H_2, that would correspond to 100% relative H_2 production. Note that with this definition it is possible, for structures containing additives, to have a relative H_2 concentration above 100%, since some of the additives may also give up hydrogen and contribute towards hydrogen production.

To give a perspective on the data itself, in total 1448 structures were generated among all 12 combinations of borohydride and additive. The points shown in Fig. 3 are the 17 best structures out of 83 total structures produced over eight generations specifically for $Al(BH_4)_3 \cdot NH_3$ (at each generation, USPEX typically records two or even more best structures, leading to 17 structures from eight generations). Of these 17 structures plotted, eight have 0% relative H_2 concentration, and, at least in terms of molecular composition, are nearly identical to the initial starting structure. Conceptually, when a structure is perturbed along a given direction—e.g., given by a soft eigenmode—and then relaxed, the system may simply revert back to a state nearly identical to its unperturbed state if the perturbation is not large enough. Because metadynamics naturally induces stronger perturbations in later generations (as the Gaussian energy penalty has been allowed to accumulate), it becomes more likely to observe states dissimilar to the ground-state structure. For the same reason, in systems with relatively-high-energy metastable states, it often takes several generations to observe structures notably dissimilar to the initial ground-state structure.

Looking at the spread of the points in Fig. 3, it is clear that, near a given hydrogen concentration, there are often several metastable states with a relatively large range in energy. From our observations, this range in energy is due to a variety of structural changes, including differences in volume, molecular composition (e.g., one structure may have more BH_3 and BH_5 units than others), or differences in molecule positions. However, our interest lies in the most stable structure at a given amount of hydrogen produced. We thus postulate that—in order to produce this amount of hydrogen—going through this state, per the Bell–Evans–Polanyi principle, is likely the most favorable pathway. Because our primary interest lies in structures that produce H_2, and furthermore only the most energetically favorable ones, we focus on the bottom half of the convex hull, as indicated by the purple line in Fig. 3. As such, all following plots only show the convex hull for the various borohydrides and additives.

C. H_2 production

Throughout the generation of metastable states using metadynamics, we found many structures with interesting physical properties, including structures with formation of ions or metal ammine complexes [67–69]—in the Supplemental Material [70] we provided both the structures and corresponding energies for the best individuals from all combinations studied. However, to study hydrogen production we henceforth restrict our analysis to the bottom half of the convex hull. Applying the procedure from the previous section, we get an estimate for the energetic cost of hydrogen production for all of the possible borohydride-additive combinations studied; the results are depicted in Fig. 4, which shows the most pertinent results of our study. Note that the y axes of all plots have been shifted so that the initial structure of each is defined to have an energy of 0 eV/BH_4, allowing for a direct comparison of the relative cost of forming hydrogen among different additives. In Fig. 5 we provide the same information as in Fig. 4, but we use an alternative y-axis scaling for use in hydrogen-storage contexts; here the total energy is not normalized by the total number of BH_4 units but by the current amount of H_2 produced, so that it shows the incremental cost to hydrogen production.

A general trend is immediately obvious from Fig. 4: Structures which contain more H_2 have, with a few exceptions,

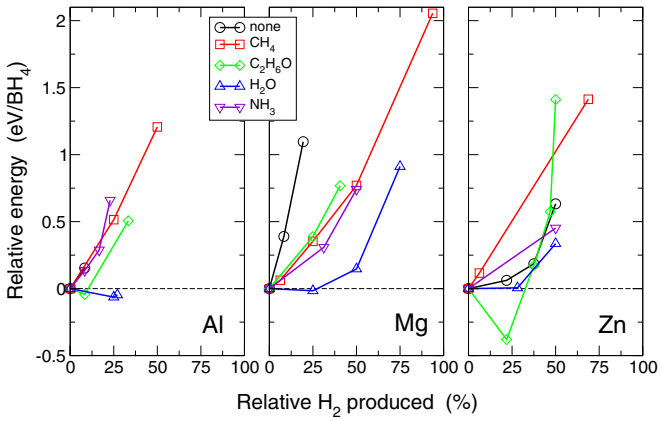

FIG. 4. Plot of energy vs relative H_2 production for all additives and structures found in the structure search lying along the bottom hull for $Al(BH_4)_3$, $Mg(BH_4)_2$, and $Zn(BH_4)_2$.

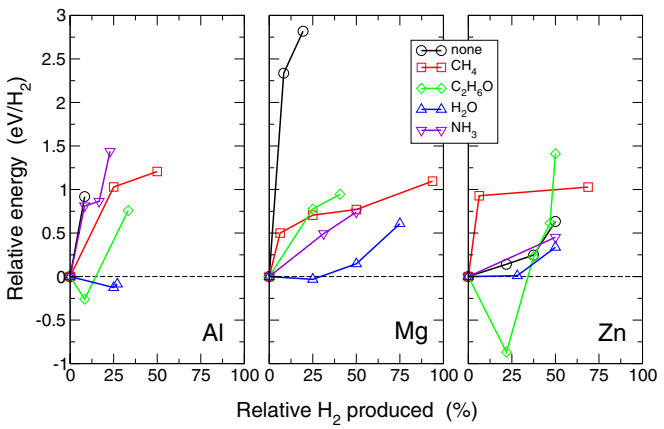

FIG. 5. Same data as Fig. 4, except that the y axis is in units of eV/H_2 produced, showing the incremental cost of hydrogen production.

a higher relative energy. This is to be expected, because it takes energy to release the hydrogen molecules. However, it is interesting to see that the curves concave upward, meaning that the initial hydrogen release seems to hinder, rather than facilitate, additional hydrogen release. Furthermore, note that, in exception to the general trend, a few structures decrease in relative energy when releasing hydrogen, signifying that the initial structure is a metastable state.[1] We also note that, while many total structures were analyzed via the evolutionary metadynamics technique, for certain combinations of borohydrides and additives relatively few concentrations of H_2 were obtained. For example, for unaltered $Al(BH_4)_3$, only two nonzero concentrations of H_2 were found, only one of which lay on the convex hull, leading to a total of only two data points for this structure in Fig. 4. This is likely due to the relative difficulty to produce H_2 molecules in $Al(BH_4)_3$, as seen by its relatively low H_2 production in experiment; see, e.g., Fig. 6 from Ref. [9].

We also find that the maximum amount of H_2 produced in Fig. 4 seems to vary depending on both the particular borohydride and additive used. One would expect that the maximum concentration correlates with how much hydrogen is produced during the decomposition process. Indeed, comparing with experimental thermal decomposition data for $Al(BH_4)_3$, $Mg(BH_4)_2$, and $Zn(BH_4)_2$, we find that the relative ordering of maximum hydrogen concentration corresponds to the relative experimental hydrogen production, i.e., $Al(BH_4)_3 < Mg(BH_4)_2 < Zn(BH_4)_2$ [8,9]. Along the same line, experimentally we know that the amount of H_2 produced in $Mg(BH_4)_2$ is substantially increased when complexed with NH_3 [66], which agrees qualitatively with the increase in maximum hydrogen concentration seen for $Mg(BH_4)_2 \cdot NH_3$ in Fig. 4. Finally, the same relative trends are seen for certain additives and certain metals, e.g., CH_4 is always found to have the highest H_2 concentration.

[1]This is not a flaw of the original ground-state structure search, since we required those structures to have all borohydride building blocks and additives completely intact.

Analyzing the relative energy costs for producing H_2 we see results that are expected. Notably, for $Mg(BH_4)_2$ we see that there is a significant decrease in the energy cost to produce H_2 when an additive molecule is involved, regardless of which particular molecule it is. This is not surprising, because it is known experimentally that complexing $Mg(BH_4)_2$ with NH_3 significantly decreases the temperature of hydrogen release [66], so it is plausible that complexing with other additives has a similar effect. For $Al(BH_4)_3$ and $Zn(BH_4)_2$ the effects of additive molecules are much less pronounced, with, e.g., NH_3 having approximately the same cost in energy as producing H_2; this also agrees with experimental results which find that, although $Al(BH_4)_3 \cdot 2NH_3$ evolves more H_2 than the pure borohydride, the temperature of hydrogen release is approximately the same [71]. It also agrees with the overall trend that NH_3 tends to destabilize stable borohydrides [i.e., $Mg(BH_4)_2$] while stabilizing unstable borohydrides [i.e., $Zn(BH_4)_2$ and $Al(BH_4)_3$] [66]. Here, we would like to note that experimentally many cases were studied with two or three NH_3 units per formula unit, whereas in all of our complexes there was only one additive molecule per formula unit; we argue that while the properties of the material depend upon the concentration of NH_3 (e.g., the temperature of hydrogen release tends to increase with the number of NH_3 units), the most significant factor qualitatively is whether the material has been complexed with NH_3 at all (e.g., see a study on ammine aluminum borohydride with varying concentrations of NH_3 [71]).

Comparing the various additives in Fig. 4, we find that they mostly have similar effects on the H_2 production, with the relative ordering among them differing upon which concentration and which borohydride is looked at. One interesting trend is that H_2O often has a noticeably lower energy for H_2 production than other additives. The physical reasoning for the trends is unclear. For example, we had initially expected H_2O to behave most similarly to NH_3 due to it also being a small, polar molecule. However, we see in fact that CH_4 behaves most similarly to NH_3, despite being a nonpolar molecule. The relatively low energy required to produce H_2 for borohydrides complexed with H_2O could be due to the willingness of H_2O to react with the BH_4 unit, as we see that it commonly forms

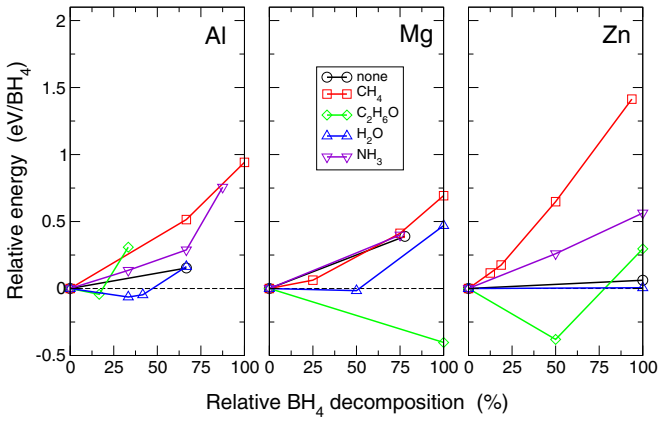

FIG. 6. Plot of energy vs relative BH_4 decomposition for all structures found in the structure search lying along the bottom hull for $Al(BH_4)_3$, $Mg(BH_4)_2$, and $Zn(BH_4)_2$, complexed with various additive molecules.

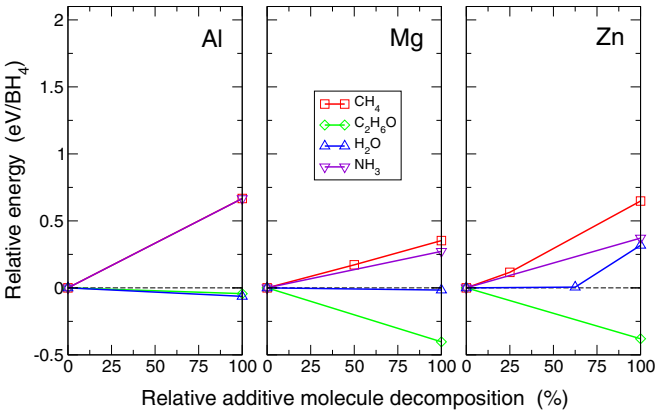

FIG. 7. Plot of energy vs relative additive molecule decomposition for all structures found in structure search lying along the bottom hull for $Al(BH_4)_3$, $Mg(BH_4)_2$, and $Zn(BH_4)_2$, complexed with various additive molecules.

BH_3–OH or BH_2–OH, leaving behind spare hydrogens to produce H_2.

We see the main value of Fig. 4 in that it provides guidance concerning which additive to choose for a given borohydride and a desired amount of hydrogen production. While the plot of course only reveals thermodynamic data of the various phases, information about the kinetic barriers can be deduced through the Bell–Evans–Polanyi principle, suggesting that lower-lying thermodynamic states also have lower barriers. One of the most promising specific findings of this study is that, of the small molecules studied, while most have effects comparable to NH_3, H_2O seems to have a significantly lower reaction pathway to produce H_2 when complexed with borohydrides. Another promising candidate is CH_4, which has effects very similar effects to those of NH_3, although it consistently evolves more H_2, as seen in Fig. 4. It is interesting to note that, while the success of NH_3 as an additive is thought to be largely due to its polarity [35,71], CH_4 sees similar results here despite the fact that it is nonpolar.

In summary, our metadynamics results suggest that the response of a borohydride to additives depends on where it falls along the "stability line," a well-known phenomenon related to the electronegativity of the borohydride's metal [8,9]—and more accurately described by its formation enthalpy [63]: Borohydrides to the right of the stability line, e.g., $Mg(BH_4)_2$, are known not to produce diborane and have their temperature of hydrogen release lowered when complexed with NH_3, whereas borohydrides to the left of the stability line, i.e., $Al(NH_4)_3$ and $Zn(BH_4)_2$, are known to produce diborane and are generally known to have their temperature of hydrogen release increased when complexed with NH_3. More stable borohydrides are less willing thermodynamically to be complexed with additives, but see a more pronounced effect in the amount of H_2 produced, whereas in less stable borohydrides additives tend to suppress the production of unwanted byproducts (i.e., B_2H_6) by stabilizing the material, although they do not see as impressive results in lowering the hydrogen release temperature.

D. BH_4 and additive decomposition

To gain further insight, we also studied the relative energy cost to decompose the BH_4 units in Fig. 6 and the additive molecules in Fig. 7—for ease of comparison, Figs. 4, 6, and 7 have the same y-axis scaling. The meaning of the x axis for these plots is comparable to that in Fig. 4, except that it is for molecule decomposition instead of formation. For example, 75% relative decomposition of BH_4 in a $2 \times 2 \times 2$ supercell of $Al(BH_4)_3$ tells us that—out of the 24 total BH_4 units—18 were decomposed and six were found intact. The primary use of Figs. 6 and 7 is to provide additional information and context to understanding the decomposition and hydrogen release processes for the various structures. These plots also help us to understand where the released hydrogen comes from, i.e., the borohydride units or the additive molecules. As before, these plots also reveal that some of the complexed borohydrides themselves are metastable structures, as the energy can be lowered by decomposing the borohydride units or the additive molecules; see, e.g., C_2H_6O in $Mg(BH_4)_2$ or $Zn(BH_4)_2$. This, of course, has implication for the feasibility of forming a stable complexed borohydride structure. However, it may be that these structures formed from a borohydride-additive complex, although not strictly borohydrides once the BH_4 reacts with the additive molecule, are themselves very good hydrogen storage materials, as evidenced by their low-energy pathways to release H_2.

Ideally, Figs. 4 and 6 are closely related, i.e., an increase in BH_4 decomposition should lead to additional H_2 formation, and the two would have similar energy profiles. As an example, we compare here the cases of Figs. 4 and 6 for $Zn(BH_4)_2 \cdot CH_4$: We see clearly that there is a similar increase in the energy cost to decompose BH_4 as there is to produce H_2. Of course, we do not expect the curves to be identical; it stands to reason that the energy cost to decompose BH_4 units will typically be lower than to produce the corresponding amount of H_2, because the former is (apart from the hydrogen of the additive molecule) a prerequisite for the latter to occur. As an example of undesirable behavior, we again look at Figs. 4 and 6, but now for $Mg(BH_4)_2 \cdot C_2H_6O$: We see an increase in relative energy along the lowest-energy path to produce H_2, but we

see a decrease in relative energy to decompose BH_4. This suggests that the most favorable path for $Mg(BH_4)_2 \cdot C_2H_6O$ is to decompose BH_4 (and, in fact, also C_2H_6O itself looking at Fig. 7), providing some evidence that $Mg(BH_4)_2 \cdot C_2H_6O$ may be a poor hydrogen storage candidate, due to its unwillingness to release H_2 compared with its willingness to decompose. In general, it is desirable for the curves in Figs. 6 and 7 to have energies not drastically lower than those found in Fig. 4.

We now move on to analyzing the energy cost to decompose the BH_4 units. For the pure borohydrides, by comparing Figs. 6 and 1, we find that this cost shows a clear correlation to the thermodynamic stability of the material, with pure $Zn(BH_4)_2$ having almost no thermodynamic cost to BH_4 decomposition. For the case of additives, NH_3 and CH_4 have a stabilizing effect while H_2O and C_2H_6O have a destabilizing effect. Furthermore, we find (again by comparing Figs. 6 and 1) that the relative stabilization or destabilization corresponds roughly to the stability of the borohydride, with $Mg(BH_4)_2$ experiencing anywhere from no stabilization to significant destabilization, whereas the less stable $Al(BH_4)_3$ and $Zn(BH_4)_2$ experience a range from significant stabilization to minor destabilization.

This trend of stabilizing and destabilizing can also be understood in terms of the energy cost to decompose the additive molecules in Fig. 7. Whereas NH_3 and CH_4 always have a relatively high, positive cost to decomposition, H_2O and C_2H_6O have (with one exception) consistently negative values. In fact, looking at H_2O and C_2H_6O across all plots we find that they often have negative or near-zero energy differences with respect to their starting structures, suggesting that, in many cases, the structure prefers to transition to a more energetically favorable state by having its molecular constituents react with one another. Looking in detail at some of the most favorable structures for these additives, we find that in general this involves the additive molecule reacting with the BH_4 unit; for example, in $Mg(BH_4)_2 \cdot H_2O$, we find the most favorable structure involved the reaction of H_2O and a single BH_4 molecule to form H_4BO and H_2.

V. CONCLUSIONS

The thermodynamic properties and local metastable states of complexed borohydrides were studied. In particular, we investigated $Al(BH_4)_3$, $Mg(BH_4)_2$, and $Zn(BH_4)_2$ with the additive molecules CH_4, C_2H_6O, H_2O, and NH_3. Although it is unfortunately unfeasible to fully simulate the borohydride decomposition reaction, we find that our results on local metastable states correlate well with experimental results for the full decomposition reaction, indicating that the initial steps in decomposition partially dictate the full decomposition reaction. Our results suggest that additives other than NH_3 could see similarly impressive results in improving the hydrogen-release properties of borohydrides. In particular, we find H_2O to be a promising candidate. Perhaps most promising in general is that the method we have employed here—i.e., using evolutionary metadynamics to study the local metastable states of a system combined with a structure search to provide the initial starting structures—has produced results that are both internally consistent and consistent with previous experimental and theoretical studies. We believe that this technique could prove very useful for any instance where the effects of additives (or indeed, other structural modifications) on the possible reaction pathways of a given system are desired.

ACKNOWLEDGMENT

This work was supported in full by NSF Grant No. DMR–1145968.

APPENDIX: OVERVIEW OF EVOLUTIONARY METADYNAMICS

Evolutionary metadynamics is a fairly new method, but it has already been successfully applied to find high-pressure carbon allotropes, multiple boron configurations and phase-transition pathways, and stable and metastable states for a variety of silicon-containing compounds [46,47,72]. Metadynamics itself allows for a sampling of rare events by adding cumulative Gaussian energy penalties to regions of phase space that have already been explored. However, care must be taken when choosing these so-called *collective variables*, i.e., the variables to which an energy penalty is added. One well-known technique for sampling nearby metastable states for a known stable structure is to use the unit cell's size and shape as the collective variables and then using molecular dynamics (e.g., simulated annealing) in order to determine the atomic positions [73]. However, this method can result in highly disordered systems [47]. Recently, it has been found that when metadynamics is combined with an evolutionary algorithm typically seen in crystal structure prediction techniques, it is possible to generate many nearby metastable states to a given initial structure [46,47]. This is done by using the unit cell's shape as a collective variable, but instead of using molecular dynamics to relax atoms within the cell, the vibrational modes of the system are used as a means of providing the evolutionary variation operators. While metadynamics itself has been developed over a decade ago [74], the evolutionary approach is still relatively new.

The method proceeds as follows: First, the user provides a reference structure (ideally the ground-state structure) and the Gaussian penalty height and width. Then, the vibrational eigenvectors and corresponding frequencies are solved for, providing a means to perturb the system, with the magnitude of the perturbation dependent on the chosen Gaussian height and width; the underlying idea here is that low activation barriers are expected to be in the direction of the lowest curvature of the free-energy landscape (i.e., the softest vibrational modes). These also serve as the evolutionary variation operators; at each generation, several structures (determined by the user) are generated using these perturbations and then partially relaxed. The best structures in that generation are then fully relaxed and may be used to produce structures for the next generation via the same process. Note that if the perturbation was too small, it relaxes back to a structure similar to the starting structure. However, if the perturbation was significant enough, it will relax to a new metastable state. Full details of this method can be found in the original works [46,47,72]. While we have also attempted other techniques, we find that combining USPEX's evolutionary algorithm with metadynamics and using constrained variables inspired by the dynamical matrix of

the ground-state structure provides a particularly efficient approach to sample many nearby low-energy metastable states.

As with any stochastic method, it is notoriously difficult to provide an estimate of error bars for the results without performing a significant amount of further calculations on the same systems to obtain more statistics. We do find that, within each generation of the metadynamics run, the energies of all structures (including those not chosen as the "best") are within a few percent of each other and variations are quite small. A source of larger variations are the random transformations that the metadynamics technique makes between generations—their effect can only be judged by repeating the same simulation many times and letting the metadynamics simulation explore as much of the phase space as possible.

[1] M. Kunowsky, J. P. Marco-Lózar, and A. Linares-Solano, J. Renew. Energy **2013**, 1 (2013).

[2] D. Durbin and C. Malardier-Jugroot, Int. J. Hydrogen Energy **38**, 14595 (2013).

[3] G. W. Crabtree, M. S. Dresselhaus, and M. V. Buchanan, Phys. Today **57**(12), 39 (2004).

[4] D. Harrison, E. Welchman, Y. J. Chabal, and T. Thonhauser, in *Energy Storage, Handbook Clean Energy Systems*, edited by J. Yan (Wiley, Hoboken, 2015), Vol. 5, pp. 2665–2683.

[5] R. Ahluwalia, T. Hua, and J. Peng, Int. J. Hydrogen Energy **37**, 2891 (2012).

[6] J. Yang, A. Sudik, C. Wolverton, and D. J. Siegel, Chem. Soc. Rev. **39**, 656 (2010).

[7] DOE Technical Targets for Onboard Hydrogen Storage for Light-Duty Vehicles, Tech. Rep. (US Department of Energy), https://www.energy.gov/eere/fuelcells/doe-technical-targets-onboard-hydrogen-storage-light-duty-vehicles.

[8] Y. Nakamori, K. Miwa, A. Ninomiya, H. Li, N. Ohba, S.-i. Towata, A. Züttel, and S.-i. Orimo, Phys. Rev. B **74**, 045126 (2006).

[9] Y. Nakamori, H.-W. Li, K. Kikuchi, M. Aoki, K. Miwa, S. Towata, and S. Orimo, J. Alloys Compd. **446**, 296 (2007).

[10] J. Graetz, Chem. Soc. Rev. **38**, 73 (2009).

[11] E. Rönnebro, Curr. Opin. Solid State Mater. Sci. **15**, 44 (2011).

[12] H.-W. Li, Y. Yan, S.-i. Orimo, A. Züttel, and C. M. Jensen, Energies (Basel, Switz.) **4**, 185 (2011).

[13] L. H. Rude, T. K. Nielsen, D. B. Ravnsbaek, U. Bösenberg, M. B. Ley, B. Richter, L. M. Arnbjerg, M. Dornheim, Y. Filinchuk, F. Besenbacher, and T. R. Jensen, Phys. Status Solidi A **208**, 1754 (2011).

[14] I. P. Jain, P. Jain, and A. Jain, J. Alloys Compd. **503**, 303 (2010).

[15] S.-i. Orimo, Y. Nakamori, J. R. Eliseo, A. Züttel, and C. M. Jensen, Chem. Rev. (Washington, DC, U.S.) **107**, 4111 (2007).

[16] T. Umegaki, J.-M. Yan, X.-B. Zhang, H. Shioyama, N. Kuriyama, and Q. Xu, Int. J. Hydrogen Energy **34**, 2303 (2009).

[17] L. George and S. K. Saxena, Int. J. Hydrogen Energy **35**, 5454 (2010).

[18] J. J. Vajo, S. L. Skeith, and F. Mertens, J. Phys. Chem. B **109**, 3719 (2005).

[19] S. V. Alapati, K. J. Johnson, and D. S. Sholl, Phys. Chem. Chem. Phys. **9**, 1438 (2007).

[20] S. V. Alapati, J. K. Johnson, and D. S. Sholl, J. Phys. Chem. C **112**, 5258 (2008).

[21] H.-W. Li, K. Kikuchi, Y. Nakamori, N. Ohba, K. Miwa, S. Towata, and S. Orimo, Acta Mater. **56**, 1342 (2008).

[22] E. A. Nickels, M. O. Jones, W. I. F. David, S. R. Johnson, R. L. Lowton, M. Sommariva, and P. P. Edwards, Angew. Chem., Int. Ed. **47**, 2817 (2008).

[23] H.-W. Li, S. Orimo, Y. Nakamori, K. Miwa, N. Ohba, S. Towata, and A. Züttel, J. Alloys Compd. **446**, 315 (2007).

[24] S. H. Lee, V. R. Manga, and Z.-K. Liu, Int. J. Hydrogen Energy **35**, 6812 (2010).

[25] M. J. van Setten, G. A. de Wijs, and G. Brocks, Phys. Rev. B **76**, 075125 (2007).

[26] H. W. Brinks, A. Fossdal, and B. C. Hauback, J. Phys. Chem. C **112**, 5658 (2008).

[27] H.-W. Li, K. Kikuchi, Y. Nakamori, K. Miwa, S. Towata, and S. Orimo, Scr. Mater. **57**, 679 (2007).

[28] H. Chu, G. Wu, Z. Xiong, J. Guo, T. He, and P. Chen, Chem. Mater. **22**, 6021 (2010).

[29] Q. Gu, L. Gao, Y. Guo, Y. Tan, Z. Tang, K. S. Wallwork, F. Zhang, and X. Yu, Energy Environ. Sci. **5**, 7590 (2012).

[30] L. H. Jepsen, M. B. Ley, Y.-S. Lee, Y. W. Cho, M. Dornheim, J. O. Jensen, Y. Filinchuk, J. E. Jørgensen, F. Besenbacher, and T. R. Jensen, Mater. Today (Oxford, U.K.) **17**, 129 (2014).

[31] E. Roedern and T. R. Jensen, Inorg. Chem. (Washington, DC, U.S.) **54**, 10477 (2015).

[32] W. Sun, X. Chen, Q. Gu, K. S. Wallwork, Y. Tan, Z. Tang, and X. Yu, Chem. - Eur. J. **18**, 6825 (2012).

[33] F. Yuan, Q. Gu, Y. Guo, W. Sun, X. Chen, and X. Yu, J. Mater. Chem. **22**, 1061 (2012).

[34] L. H. Jepsen, M. B. Ley, R. Černý, Y.-S. Lee, Y. W. Cho, D. Ravnsbæk, F. Besenbacher, J. Skibsted, and T. R. Jensen, Inorg. Chem. (Washington, DC, U.S.) **54**, 7402 (2015).

[35] E. Welchman and T. Thonhauser, J. Mater. Chem. A **5**, 4084 (2017).

[36] I. Dovgaliuk, V. Ban, Y. Sadikin, R. Černý, L. Aranda, N. Casati, M. Devillers, and Y. Filinchuk, J. Phys. Chem. C **118**, 145 (2014).

[37] K. Miwa, N. Ohba, S.-i. Towata, Y. Nakamori, A. Züttel, and S.-i. Orimo, J. Alloys Compd. **446**, 310 (2007).

[38] R. J. Newhouse, V. Stavila, S.-J. Hwang, L. E. Klebanoff, and J. Z. Zhang, J. Phys. Chem. C **114**, 5224 (2010).

[39] M. Chong, A. Karkamkar, T. Autrey, S.-i. Orimo, S. Jalisatgi, and C. M. Jensen, Chem. Commun. **47**, 1330 (2011).

[40] T. D. Huan, M. Amsler, R. Sabatini, V. N. Tuoc, N. B. Le, L. M. Woods, N. Marzari, and S. Goedecker, Phys. Rev. B **88**, 024108 (2013).

[41] G. N. Kalantzopoulos, J. G. Vitillo, E. Albanese, E. Pinatel, B. Civalleri, S. Deledda, S. Bordiga, M. Baricco, and B. C. Hauback, J. Alloys Compd. **615**, S702 (2014).

[42] G. Henkelman, B. P. Uberuaga, and H. Jónsson, J. Chem. Phys. **113**, 9901 (2000).

[43] G. Henkelman and H. Jónsson, J. Chem. Phys. **113**, 9978 (2000).

[44] Y. Yan, H.-W. Li, H. Maekawa, M. Aoki, T. Noritake, M. Matsumoto, K. Miwa, S.-i. Towata, and S.-i. Orimo, Mater. Trans. **52**, 1443 (2011).

[45] D. Frenkel and B. Smit, *Understanding Molecular Simulation: From Algorithms to Applications*, 2nd ed. (Academic Press, San Diego, 2001).
[46] Q. Zhu, A. R. Oganov, and A. O. Lyakhov, CrystEngComm **14**, 3596 (2012).
[47] Q. Zhu, A. R. Oganov, A. O. Lyakhov, and X. Yu, Phys. Rev. B **92**, 024106 (2015).
[48] R. P. Bell, Proc. R. Soc. London, Ser. A **154**, 414 (1936).
[49] M. G. Evans and M. Polanyi, Trans. Faraday Soc. **32**, 1333 (1936).
[50] G. Kresse and J. Furthmüller, Phys. Rev. B **54**, 11169 (1996).
[51] G. Kresse and D. Joubert, Phys. Rev. B **59**, 1758 (1999).
[52] Z. Łodziana, Phys. Rev. B **81**, 144108 (2010).
[53] A. Bil, B. Kolb, R. Atkinson, D. G. Pettifor, T. Thonhauser, and A. N. Kolmogorov, Phys. Rev. B **83**, 224103 (2011).
[54] T. Thonhauser, S. Zuluaga, C. A. Arter, K. Berland, E. Schröder, and P. Hyldgaard, Phys. Rev. Lett. **115**, 136402 (2015).
[55] K. Berland, V. R. Cooper, K. Lee, E. Schröder, T. Thonhauser, P. Hyldgaard, and B. I. Lundqvist, Rep. Prog. Phys. **78**, 066501 (2015).
[56] T. Thonhauser, V. R. Cooper, S. Li, A. Puzder, P. Hyldgaard, and D. C. Langreth, Phys. Rev. B **76**, 125112 (2007).
[57] D. C. Langreth, B. I. Lundqvist, S. D. Chakarova-Käck, V. R. Cooper, M. Dion, P. Hyldgaard, A. Kelkkanen, J. Kleis, L. Kong, S. Li, P. G. Moses, E. D. Murray, A. Puzder, H. Rydberg, E. Schröder, and T. Thonhauser, J. Phys.: Condens. Matter **21**, 084203 (2009).
[58] A. R. Oganov and C. W. Glass, J. Chem. Phys. **124**, 244704 (2006).
[59] A. R. Oganov, A. O. Lyakhov, and M. Valle, Acc. Chem. Res. **44**, 227 (2011).
[60] A. O. Lyakhov, A. R. Oganov, H. T. Stokes, and Q. Zhu, Comput. Phys. Commun. **184**, 1172 (2013).
[61] Q. Zhu, A. R. Oganov, C. W. Glass, and H. T. Stokes, Acta Crystallogr., Sect. B: Struct. Sci. **68**, 215 (2012).
[62] D. Harrison and T. Thonhauser, Phys. Rev. B **90**, 125152 (2014).
[63] D. Harrison and T. Thonhauser, Int. J. Hydrogen Energy **41**, 3571 (2016).
[64] S. Aldridge, A. J. Blake, A. J. Downs, S. Parsons, and C. R. Pulham, J. Chem. Soc., Dalton Trans., 853 (1996).
[65] M. J. van Setten, M. A. Uijttewaal, G. A. de Wijs, and R. A. de Groot, J. Am. Chem. Soc. **129**, 2458 (2007).
[66] G. Soloveichik, J.-H. Her, P. W. Stephens, Y. Gao, J. Rijssenbeek, M. Andrus, and J.-C. Zhao, Inorg. Chem. (Washington, DC, U.S.) **47**, 4290 (2008).
[67] L. H. Jepsen, M. B. Ley, Y. Filinchuk, F. Besenbacher, and T. R. Jensen, ChemSusChem **8**, 1452 (2015).
[68] C. H. Christensen, R. Z. Sorensen, T. Johannessen, U. J. Quaade, K. Honkala, T. D. Elmoe, R. Kohler, and J. K. Norskov, J. Mater. Chem. **15**, 4106 (2005).
[69] O. Netskina, O. Komova, S. Mukha, and V. Simagina, Catal. Commun. **85**, 9 (2016).
[70] See Supplemental Material at http://link.aps.org/supplemental/10.1103/PhysRevMaterials.2.065403 for additional details concerning the energetics, atomic coordinates, and unit-cell parameters of all structures considered in our metadynamics simulations.
[71] Y. Guo, Y. Jiang, G. Xia, and X. Yu, Chem. Commun. **48**, 4408 (2012).
[72] Q. Zhu, Q. Zeng, and A. R. Oganov, Phys. Rev. B **85**, 201407 (2012).
[73] R. Martoňák, A. Laio, and M. Parrinello, Phys. Rev. Lett. **90**, 075503 (2003).
[74] A. Laio and M. Parrinello, Proc. Natl. Acad. Sci. U.S.A. **99**, 12562 (2002).